International Journal of Solids and Structures 50 (2013) 1916–1929

Contents lists available at SciVerse ScienceDirect

International Journal of Solids and Structures

journal homepage: www.elsevier.com/locate/ijsolstr

# Three-dimensional exact analysis of piezoelectric laminated plates via a sampling surfaces method

G.M. Kulikov *, S.V. Plotnikova

*Department of Applied Mathematics and Mechanics, Tambov State Technical University, Sovetskaya Street, 106, Tambov 392000, Russia*

ARTICLE INFO

*Article history:*
Received 24 November 2012
Received in revised form 9 February 2013
Available online 26 February 2013

*Keywords:*
Piezoelectric laminated plate
3D exact solutions
Cross-ply composite
Antisymmetric angle-ply composite
Sampling surfaces method

ABSTRACT

A paper focuses on the use of the efficient approach to three-dimensional (3D) exact solutions of electroelasticity for piezoelectric laminated plates. This approach is based on the new method of sampling surfaces (SaS) developed recently by the authors. We introduce inside the $n$th layer $I_n$ not equally spaced SaS parallel to the middle surface of the plate and choose displacements of these surfaces as basic plate variables. Such an idea permits the representation of the proposed piezoelectric plate formulation in a very compact form. This fact gives the opportunity to derive the 3D exact solutions of electroelasticity for thick and thin piezoelectric laminated plates with a specified accuracy utilizing a sufficient number of SaS, which are located at interfaces and Chebyshev polynomial nodes.



## 1. Introduction

Three-dimensional (3D) static analysis of piezoelectric laminated plates has received considerable attention during past twenty years. In this respect, the cross-ply lay-up was until very recently the most complicated material configuration for which relevant 3D analytical solutions were available in the literature (see, e.g. survey papers of Tauchert et al., 2000; Wu et al., 2008). As it is known, there are three different approaches to 3D exact solutions of electroelasticity for piezoelectric laminated plates, namely, the Pagano approach, the state space approach and the asymptotic approach. The first approach (Vlasov, 1957; Pagano, 1969, 1970a,b) was implemented for piezoelectric plates by Ray et al. (1992, 1993), Heyliger (1994, 1997), Heyliger and Brooks (1996), Kapuria et al. (1999). The most popular state space approach was extensively utilized by Lee and Jiang (1996), Bisegna and Maceri (1996), Benjeddou and Deú (2001), Vel and Batra (2000a,b), Tarn (2002), Zhong and Shang (2003). The 3D electroelasticity solutions based on the asymptotic series expansion were obtained in contributions of Cheng and Batra (2000), Cheng et al. (2000), Kalamkarov and Kolpakov (2001), Reddy and Cheng (2001), Vetyukov et al. (2011). However, 3D exact solutions for piezoelectric laminated plates of general lay-up configurations cannot be found in the current literature; only developments for antisymmetric angle-ply laminates in the framework of 3D anisotropic elasticity are available (Noor and Burton, 1990; Savoia and Reddy, 1992; Kulikov and Plotnikova, 2012a).

To solve such a problem, we invoke a new efficient method of sampling surfaces (SaS) proposed recently for single-layer shells (Kulikov and Plotnikova, 2011b, 2012b) and laminated plates and shells (Kulikov and Plotnikova, 2012a, 2013). As SaS denoted by $\Omega^{(n)1}, \Omega^{(n)2}, \ldots, \Omega^{(n)I_n}$, we choose outer surfaces and any inner surfaces inside the $n$th layer and introduce displacement vectors $\mathbf{u}^{(n)1}, \mathbf{u}^{(n)2}, \ldots, \mathbf{u}^{(n)I_n}$ of these surfaces as basic plate variables, where $I_n$ is the total number of SaS chosen for each layer ($I_n \geqslant 3$). Such choice of displacements with the consequent use of Lagrange polynomials of degree $I_n - 1$ in the thickness direction for each layer permits the representation of governing equations of the piezoelectric laminated plate in a very compact form. It is necessary to note that the term SaS should not be confused with such terms as fictitious interfaces or virtual interfaces, which are extensively used in layer-wise theories. The main difference consists in the lack of possibility to employ the polynomials of high degree in the thickness direction because in conventional layer-wise theories only the third and fourth order polynomial interpolations are admissible (see, e.g. Carrera, 2002, 2003; Carrera et al., 2011). This restricts the use of the fictitious/virtual interfaces technique for derivation of 3D exact elasticity solutions. On the contrary, the SaS method permits the use of polynomials of high degree. This fact gives in turn the opportunity to derive 3D exact solutions for laminated composite plates with a prescribed accuracy employing a sufficiently large number of not equally spaced SaS.

It is important to mention that the developed approach with equally spaced SaS (Kulikov and Plotnikova, 2011b) does not work properly with Lagrange polynomials of high degree because the Runge's phenomenon can occur, which yields the wild oscillation at the edges of the interval when the user deals with any specific

* Corresponding author.
*E-mail addresses:* kulikov@apmath.tstu.ru, gmkulikov@mail.ru (G.M. Kulikov).

0020-7683/$ - see front matter © 2013 Elsevier Ltd. All rights reserved.
http://dx.doi.org/10.1016/j.ijsolstr.2013.02.015

functions. If the number of equally spaced nodes is increased then the oscillations become even larger. Fortunately, the use of Chebyshev polynomial nodes (Burden and Faires, 2010) can help to improve significantly the behavior of Lagrange polynomials of high degree for which the error will go to zero as $I_n \to \infty$.

The present paper is also intended to show that the SaS method can be applied efficiently to the solution of aforementioned problems. The authors restrict themselves to finding *five right digits* in all examples presented. The better accuracy is possible of course but requires more SaS inside each layer to be taken.

## 2. Three dimensional description of laminated plate

Consider a piezoelectric laminated plate of the thickness $h$. Let the middle surface $\Omega$ be described by Cartesian coordinates $x_1$ and $x_2$. The coordinate $x_3$ is oriented in the thickness direction. The transverse coordinates of SaS inside the $n$th layer are defined as

$$x_3^{(n)1} = x_3^{[n-1]}, \quad x_3^{(n)I_n} = x_3^{[n]},$$

$$x_3^{(n)m_n} = \frac{1}{2}\left(x_3^{[n-1]} + x_3^{[n]}\right) - \frac{1}{2}h_n \cos\left(\pi \frac{2m_n - 3}{2(I_n - 2)}\right), \tag{1}$$

where $x_3^{[n-1]}$ and $x_3^{[n]}$ are the transverse coordinates of layer interfaces $\Omega^{[n-1]}$ and $\Omega^{[n]}$ (Fig. 1); $h_n = x_3^{[n]} - x_3^{[n-1]}$ is the thickness of the $n$th layer; the index $n$ identifies the belonging of any quantity to the $n$th layer and runs from 1 to $N$, where $N$ is the number of layers; the index $m_n$ identifies the belonging of any quantity to inner SaS of the $n$th layer and runs from 2 to $I_n - 1$ , whereas the indices $i_n$ , $j_n$, $k_n$ to be introduced later for describing all SaS of the $n$th layer run from 1 to $I_n$.

**Remark 1.** It is worth noting that transverse coordinates of inner SaS (1) coincide with coordinates of Chebyshev polynomial nodes (Burden and Faires, 2010). This fact has a great meaning for a convergence of the SaS method.

The strain tensor is given by

$$2\varepsilon_{ij} = u_{i,j} + u_{j,i}, \tag{2}$$

where $u_i$ are the displacements of the plate. Here and in the following developments, Latin indices $i, j, k, \ell$ range from 1 to 3 while Greek indices $\alpha, \beta$ range from 1 to 2.

The strain components at SaS can be written as

$$2\varepsilon_{\alpha\beta}^{(n)i_n} = 2\varepsilon_{\alpha\beta}\left(x_3^{(n)i_n}\right) = u_{\alpha,\beta}^{(n)i_n} + u_{\beta,\alpha}^{(n)i_n},$$

$$2\varepsilon_{\alpha 3}^{(n)i_n} = 2\varepsilon_{\alpha 3}\left(x_3^{(n)i_n}\right) = \beta_\alpha^{(n)i_n} + u_{3,\alpha}^{(n)i_n},$$

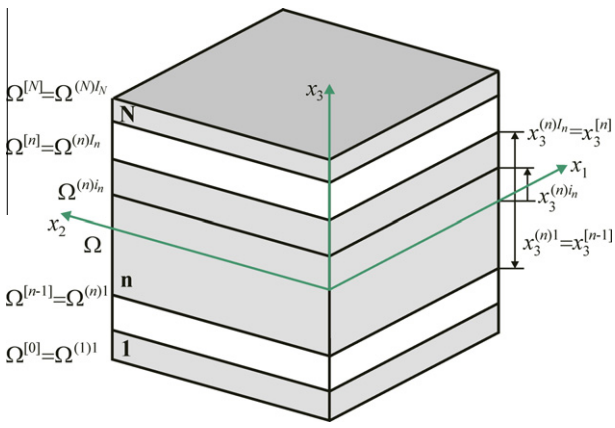


**Fig. 1.** Geometry of the laminated plate.

$$\varepsilon_{33}^{(n)i_n} = \varepsilon_{33}\left(x_3^{(n)i_n}\right) = \beta_3^{(n)i_n}, \tag{3}$$

where $u_i^{(n)i_n}(x_1, x_2)$ are the displacements of SaS of the $n$th layer; $\beta_i^{(n)i_n}(x_1, x_2)$ are the values of derivatives of displacements with respect to coordinate $x_3$ at SaS, that is,

$$u_i^{(n)i_n} = u_i\left(x_3^{(n)i_n}\right), \quad \beta_i^{(n)i_n} = u_{i,3}\left(x_3^{(n)i_n}\right). \tag{4}$$

Next, we assume that displacements are distributed through the thickness of the $n$th layer as follows:

$$u_i^{(n)} = \sum_{i_n} L^{(n)i_n} u_i^{(n)i_n}, \quad x_3^{[n-1]} \leqslant x_3 \leqslant x_3^{[n]}, \tag{5}$$

where $L^{(n)i_n}(x_3)$ are the Lagrange polynomials of degree $I_n - 1$ expressed as

$$L^{(n)i_n} = \prod_{j_n \neq i_n} \frac{x_3 - x_3^{(n)j_n}}{x_3^{(n)i_n} - x_3^{(n)j_n}}. \tag{6}$$

The use of (4) and (5) yields

$$\beta_i^{(n)i_n} = \sum_{j_n} M^{(n)j_n}\left(x_3^{(n)i_n}\right) u_i^{(n)j_n}, \tag{7}$$

where $M^{(n)j_n} = L_{,3}^{(n)j_n}$ are the derivatives of Lagrange polynomials, which are calculated at SaS of the $n$th layer as

$$M^{(n)j_n}\left(x_3^{(n)i_n}\right) = \frac{1}{x_3^{(n)j_n} - x_3^{(n)i_n}} \prod_{k_n \neq i_n, j_n} \frac{x_3^{(n)i_n} - x_3^{(n)k_n}}{x_3^{(n)j_n} - x_3^{(n)k_n}} \quad \text{for} \quad j_n \neq i_n,$$

$$M^{(n)i_n}\left(x_3^{(n)i_n}\right) = -\sum_{j_n \neq i_n} M^{(n)j_n}\left(x_3^{(n)i_n}\right). \tag{8}$$

Thus, the key functions $\beta_i^{(n)i_n}$ of the proposed plate formulation are represented according to (7) as *a linear combination* of displacements of SaS of the $n$th layer $u_i^{(n)j_n}$.

The following step consists in a choice of consistent approximation of strains through the thickness of the $n$th layer. It is apparent that the strain distribution should be chosen similar to the displacement distribution (5):

$$\varepsilon_{ij}^{(n)} = \sum_{i_n} L^{(n)i_n} \varepsilon_{ij}^{(n)i_n}, \quad x_3^{[n-1]} \leqslant x_3 \leqslant x_3^{[n]}. \tag{9}$$

## 3. Description of electric field

The relation between the electric field and the electric potential $\varphi$ is given by

$$E_i = -\varphi_{,i}. \tag{10}$$

The electric field vector at SaS of the $n$th layer is written as

$$E_\alpha^{(n)i_n} = E_\alpha\left(x_3^{(n)i_n}\right) = -\varphi_{,\alpha}^{(n)i_n}, \tag{11}$$

$$E_3^{(n)i_n} = E_3\left(x_3^{(n)i_n}\right) = -\psi^{(n)i_n}, \tag{12}$$

where $\varphi^{(n)i_n}(x_1, x_2)$ are the electric potentials of SaS of the $n$th layer; $\psi^{(n)i_n}(x_1, x_2)$ are the values of the derivative of the electric potential with respect to thickness coordinate at SaS, that is,

$$\varphi^{(n)i_n} = \varphi\left(x_3^{(n)i_n}\right), \quad \psi^{(n)i_n} = \varphi_{,3}\left(x_3^{(n)i_n}\right). \tag{13}$$

Following a proposed SaS technique, we assume that the electric potential and the electric field vector are distributed through the thickness of the $n$th layer by

$$\varphi^{(n)} = \sum_{i_n} L^{(n)i_n} \varphi^{(n)i_n}, \quad x_3^{[n-1]} \leqslant x_3 \leqslant x_3^{[n]}, \tag{14}$$

$$E_i^{(n)} = \sum_{i_n} L^{(n)i_n} E_i^{(n)i_n}, \quad x_3^{[n-1]} \leqslant x_3 \leqslant x_3^{[n]}. \tag{15}$$

The use of (13) and (14) leads to a simple formula

$$\psi^{(n)i_n} = \sum_{j_n} M^{(n)j_n}\left(x_3^{(n)i_n}\right)\varphi^{(n)j_n}, \tag{16}$$

which is similar to (7). This implies that the key functions $\psi^{(n)i_n}$ of the piezoelectric plate formulation are represented as a linear combination of electric potentials of SaS of the $n$th layer $\varphi^{(n)j_n}$.

## 4. Variational formulation

The extended potential energy of the piezoelectric laminated plate (Tzou, 1993) can be written as follows:

$$\Pi = \frac{1}{2}\iint_{\Omega}\sum_n \int_{x_3^{[n-1]}}^{x_3^{[n]}} \left(\sum_{i,j}\sigma_{ij}^{(n)}\varepsilon_{ij}^{(n)} - \sum_i D_i^{(n)}E_i^n\right)dx_1dx_2dx_3 - W, \tag{17}$$

$$W = \iint_{\Omega}\left[\sum_i\left(p_i^+u_i^{[N]} - p_i^-u_i^{[0]}\right) - q^+\varphi^{[N]} - q^-\varphi^{[0]}\right]dx_1dx_2 + W_{\sum}, \tag{18}$$

where $\sigma_{ij}^{(n)}$ is the stress tensor of the $n$th layer; $D_i^{(n)}$ is the electric displacement vector of the $n$th layer; $u_i^{[0]} = u_i^{(1)1}$ and $u_i^{[N]} = u_i^{(N)I_N}$ are the displacements of bottom and top surfaces $\Omega^{[0]}$ and $\Omega^{[N]}$; $\varphi^{[0]} = \varphi^{(1)1}$ and $\varphi^{[N]} = \varphi^{(N)I_N}$ are the electric potentials of bottom and top surfaces; $p_i^-$ and $p_i^+$ are the loads acting on outer surfaces; $q^-$ and $q^+$ are the electric charges on outer surfaces; $W_\Sigma$ is the work done by external electromechanical loads applied to the boundary surface $\Sigma$.

**Table 1**
Elastic, piezoelectric and dielectric properties of materials.

| Material | PVDF | PZT-5A | PZT | Gr/Ep |
|---|---|---|---|---|
| $C_{1111}$, GPa | 238.0 | 99.201 | 84.8 | 183.443 |
| $C_{2222}$, GPa | 23.6 | 99.201 | 84.8 | 11.662 |
| $C_{3333}$, GPa | 10.6 | 86.856 | 84.8 | 11.662 |
| $C_{1122}$, GPa | 3.98 | 54.016 | 36.3 | 4.363 |
| $C_{1133}$, GPa | 2.19 | 50.778 | 36.3 | 4.363 |
| $C_{2233}$, GPa | 1.92 | 50.778 | 36.3 | 3.918 |
| $C_{2323}$, GPa | 2.15 | 21.1 | 24.23 | 2.87 |
| $C_{1313}$, GPa | 4.40 | 21.1 | 24.23 | 7.17 |
| $C_{1212}$, GPa | 6.43 | 22.593 | 24.23 | 7.17 |
| $e_{311}$, C/m$^2$ | −0.13 | −7.209 | 21.677 | 0 |
| $e_{322}$, C/m$^2$ | −0.14 | −7.209 | 21.677 | 0 |
| $e_{333}$, C/m$^2$ | −0.28 | 15.118 | 12.995 | 0 |
| $e_{223}$, C/m$^2$ | −0.01 | 12.322 | 0 | 0 |
| $e_{113}$, C/m$^2$ | −0.01 | 12.322 | 0 | 0 |
| $\in_{11}$, nF/m | 0.11068 | 15.3 | 16.5 | 15.3 |
| $\in_{22}$, nF/m | 0.10607 | 15.3 | 16.5 | 15.3 |
| $\in_{33}$, nF/m | 0.10607 | 15.0 | 16.5 | 15.3 |

Substituting strain and electric field distributions (9) and (15) in (17) and introducing stress resultants

$$H_{ij}^{(n)i_n} = \int_{x_3^{[n-1]}}^{x_3^{[n]}} \sigma_{ij}^{(n)}L^{(n)i_n}dx_3 \tag{19}$$

and electric displacement resultants

$$T_i^{(n)i_n} = \int_{x_3^{[n-1]}}^{x_3^{[n]}} D_i^{(n)}L^{(n)i_n}dx_3, \tag{20}$$

one obtains

$$\prod = \frac{1}{2}\iint_{\Omega}\sum_n\sum_{i_n}\left(\sum_{i,j}H_{ij}^{(n)i_n}\varepsilon_{ij}^{(n)i_n} - \sum_i T_i^{(n)i_n}E_i^{(n)i_n}\right)dx_1dx_2 - W. \tag{21}$$

For simplicity, we consider the case of linear piezoelectric materials described as

$$\sigma_{ij}^{(n)} = \sum_{k,\ell}C_{ijk\ell}^{(n)}\varepsilon_{k\ell}^{(n)} - \sum_k e_{kij}^{(n)}E_k^{(n)}, \quad x_3^{[n-1]} \leqslant x_3 \leqslant x_3^{[n]}, \tag{22}$$

$$D_i^{(n)} = \sum_{k,\ell}e_{ik\ell}^{(n)}\varepsilon_{k\ell}^{(n)} + \sum_k \in_{ik}^{(n)}E_k^{(n)}, \quad x_3^{[n-1]} \leqslant x_3 \leqslant x_3^{[n]}, \tag{23}$$

where $C_{ijkl}^{(n)}$, $e_{kij}^{(n)}$ and $\in_{ij}^{(n)}$ are the elastic, piezoelectric and dielectric constants of the $n$th layer.

Inserting (22) and (23) correspondingly in (19) and (20) and taking into account strain and electric field distributions (9) and (15), we have

$$H_{ij}^{(n)i_n} = \sum_{j_n}\Lambda^{(n)i_nj_n}\left(\sum_{k,\ell}C_{ijk\ell}^{(n)}\varepsilon_{k\ell}^{(n)j_n} - \sum_k e_{kij}^{(n)}E_k^{(n)j_n}\right), \tag{24}$$

$$T_i^{(n)i_n} = \sum_{j_n}\Lambda^{(n)i_nj_n}\left(\sum_{k,\ell}e_{ik\ell}^{(n)}\varepsilon_{k\ell}^{(n)j_n} + \sum_k \in_{ik}^{(n)}E_k^{(n)j_n}\right), \tag{25}$$

where

$$\Lambda^{(n)i_nj_n} = \int_{x_3^{[n-1]}}^{x_3^{[n]}} L^{(n)i_n}L^{(n)j_n}dx_3. \tag{26}$$

Now, the variational equation for the piezoelectric laminated plate in the case of conservative loading is written as

$$\delta\Pi = 0. \tag{27}$$

**Remark 2.** The proposed 3D variational formulation generalizes 6- and 9- parameter formulations for piezoelectric structures based on using the displacements of respectively two and three SaS (Kulikov and Plotnikova, 2008, 2011a).

**Table 2**
Results for a piezoelectric three-ply plate with $a/h = 4$ under mechanical loading[a]

| Variable | Exact | $I_n = 3$ | $I_n = 5$ | $I_n = 7$ | $I_n = 9$ | $I_n = 11$ |
|---|---|---|---|---|---|---|
| $-u_1(0, a/2, 0.005) \times 10^{12}$, m | 1.719 | 1.6879 | 1.7188 | 1.7188 | 1.7188 | 1.7188 |
| $u_3(a/2, a/2, 0.005) \times 10^{11}$, m | 1.529 | 1.5170 | 1.5285 | 1.5285 | 1.5285 | 1.5285 |
| $\sigma_{11}(a/2, a/2, 0.005) \times 10^{-1}$, Pa | 3.371 | 3.3158 | 3.3715 | 3.3714 | 3.3714 | 3.3714 |
| $-\sigma_{12}(0, 0, 0.005)$, Pa | 2.639 | 2.6030 | 2.6391 | 2.6391 | 2.6391 | 2.6391 |
| $\sigma_{13}(0, a/2, 0.0023)$, Pa | 3.081 | 3.1722 | 3.0697 | 3.0790 | 3.0789 | 3.0789 |
| $\sigma_{23}(a/2, 0, 0)$, Pa | 2.614 | 2.2396 | 2.6216 | 2.6139 | 2.6140 | 2.6140 |
| $\varphi(a/2, a/2, 0) \times 10^3$, V | 1.280 | 1.2707 | 1.2798 | 1.2798 | 1.2798 | 1.2798 |
| $-D_1(0, a/2, 0) \times 10^{11}$, C/m$^2$ | 2.414 | 2.3888 | 2.4139 | 2.4138 | 2.4138 | 2.4138 |
| $-D_3(a/2, a/2, 0.005) \times 10^{11}$, C/m$^2$ | 4.970 | 5.4455 | 4.9770 | 4.9697 | 4.9696 | 4.9696 |

[a] Exact results are given by Lage et al. (2004).

## 5. 3D exact solution for piezoelectric laminated orthotropic plates

In this section, we study a simply supported piezoelectric laminated orthotropic rectangular plate. The edge boundary conditions of the plate are assumed to be fully supported and electrically grounded, that is,

$$\begin{aligned} &\sigma_{11}^{(n)} = u_2^{(n)} = u_3^{(n)} = \varphi^{(n)} = 0 \quad \text{at } x_1 = 0 \text{ and } x_1 = a, \\ &\sigma_{22}^{(n)} = u_1^{(n)} = u_3^{(n)} = \varphi^{(n)} = 0 \quad \text{at } x_2 = 0 \text{ and } x_2 = b, \end{aligned} \tag{28}$$

where $a$ and $b$ are the plate dimensions. To satisfy boundary conditions, we search an analytical solution of the problem by a method of double Fourier series expansion

**Table 3**
Results for a piezoelectric three-ply plate with $a/h = 10$ under mechanical loading[b].

| Variable | Exact | $I_n = 3$ | $I_n = 5$ | $I_n = 7$ | $I_n = 9$ |
|---|---|---|---|---|---|
| $u_1(0, a/2, -0.005) \times 10^{11}$, m | 2.085 | 2.0820 | 2.0851 | 2.0851 | 2.0851 |
| $u_3(a/2, a/2, 0.00417) \times 10^{10}$, m | 2.121 | 2.1185 | 2.1210 | 2.1210 | 2.1210 |
| $\sigma_{11}(a/2, a/2, 0.005) \times 10^{-2}$, Pa | 1.594 | 1.5918 | 1.5938 | 1.5938 | 1.5938 |
| $\sigma_{12}(0, 0, -0.005) \times 10^{-1}$, Pa | 1.023 | 1.0218 | 1.0232 | 1.0232 | 1.0232 |
| $\sigma_{13}(0, a/2, 0) \times 10^{-1}$, Pa | 1.004 | 0.9978 | 1.0045 | 1.0045 | 1.0045 |
| $\sigma_{23}(a/2, 0, 0)$, Pa | 4.265 | 3.6243 | 4.2666 | 4.2645 | 4.2645 |
| $\varphi(a/2, a/2, 0) \times 10^3$, V | 3.462 | 3.4572 | 3.4617 | 3.4617 | 3.4617 |
| $-D_1(0, a/2, 0) \times 10^{11}$, C/m$^2$ | 5.826 | 5.7933 | 5.8261 | 5.8261 | 5.8261 |
| $-D_3(a/2, a/2, 0.005) \times 10^{11}$, C/m$^2$ | 4.676 | 5.1090 | 4.6773 | 4.6759 | 4.6759 |

[b] Exact results are given by Lage et al. (2004).

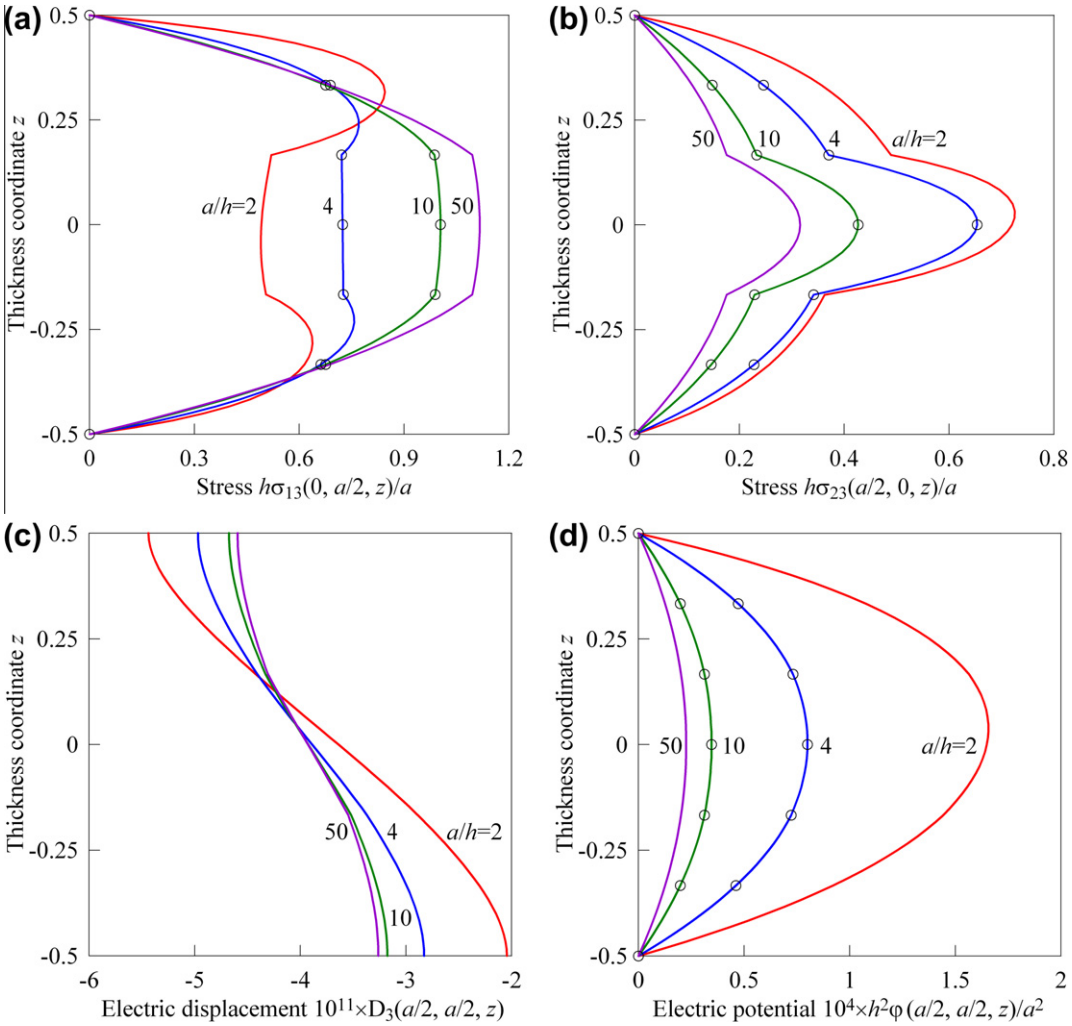


**Fig. 2.** Distributions of transverse shear stresses, electric displacement and electric potential through the thickness of the three-ply plate subjected to mechanical loading for $I_1 = I_2 = I_3 = 7$: present analysis (—) and Heyliger (○), where $z = x_3/h$.

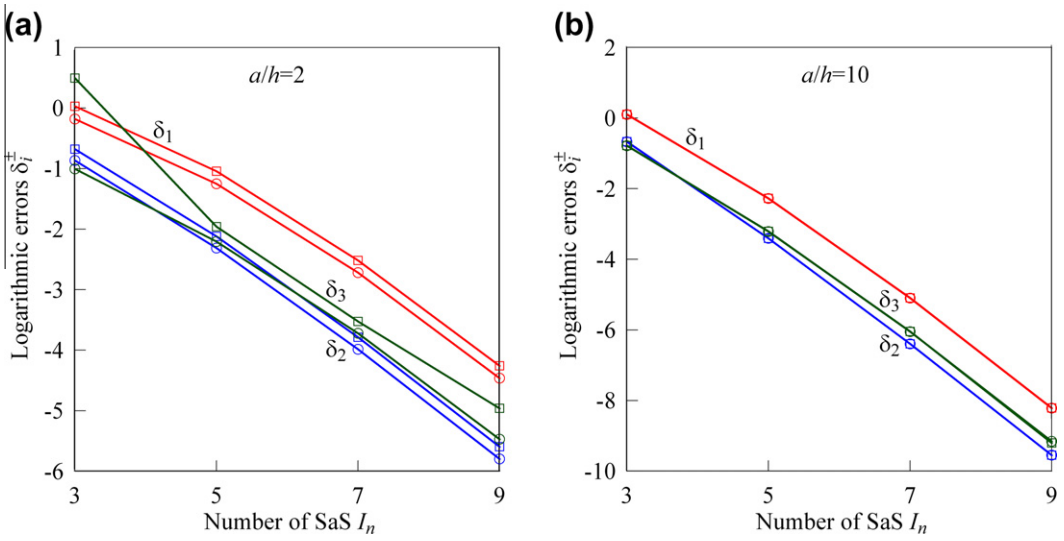


**Fig. 3.** Accuracy of satisfying the boundary conditions $\delta_i^-$ and $\delta_i^+$ on the bottom (○) and top (□) surfaces of the three-ply plate: (a) $a/h = 2$ and (b) $a/h = 10$.

$$
\begin{aligned}
u_1^{(n)i_n} &= \sum_{r,s} \overline{u}_{1rs}^{(n)i_n} \cos\frac{r\pi x_1}{a} \sin\frac{s\pi x_2}{b},\\
u_2^{(n)i_n} &= \sum_{r,s} \overline{u}_{2rs}^{(n)i_n} \sin\frac{r\pi x_1}{a} \cos\frac{s\pi x_2}{b},\\
u_3^{(n)i_n} &= \sum_{r,s} \overline{u}_{3rs}^{(n)i_n} \sin\frac{r\pi x_1}{a} \sin\frac{s\pi x_2}{b},\\
\varphi^{(n)i_n} &= \sum_{r,s} \overline{\varphi}_{rs}^{(n)i_n} \sin\frac{r\pi x_1}{a} \sin\frac{s\pi x_2}{b},
\end{aligned}
\tag{29}
$$

where $r, s \in N$. The external electromechanical loads are also expanded in double Fourier series.

Substituting (29) and Fourier series corresponding to electromechanical loading into the extended potential energy (18) and (21) with $W_\Sigma = 0$ and allowing for (3), (7), (11), (12), (16), (24), and (25), one obtains

$$
\Pi = \sum_{r,s} \Pi_{rs}\left(\overline{u}_{irs}^{(n)i_n},\ \overline{\varphi}_{rs}^{(n)i_n}\right). \tag{30}
$$

Invoking further the variational equation (27), we arrive at the system of linear algebraic equations

$$
\frac{\partial \Pi_{rs}}{\partial \overline{u}_{irs}^{(n)i_n}} = 0, \quad \frac{\partial \Pi_{rs}}{\partial \overline{\varphi}_{rs}^{(n)i_n}} = 0 \tag{31}
$$

of order $4\left(\sum_n I_n - N + 1\right)$. The linear system (31) can be easily solved by using a method of Gaussian elimination.

The described algorithm was performed with the Symbolic Math Toolbox, which incorporates symbolic computations into the numeric environment of MATLAB. The latter gave the possibility to derive the exact solutions of 3D electroelasticity for laminated orthotropic plates with a specified accuracy.

### 5.1. Square piezoelectric three-layer plate under mechanical loading

Consider a square plate subjected to the transverse load

$$
p_1^- = p_1^+ = p_2^- = p_2^+ = p_3^- = 0, \quad p_3^+ = p_0 \sin\frac{\pi x_1}{a} \sin\frac{\pi x_2}{b}. \tag{32}
$$

The symmetric three-ply laminate with the stacking sequence [0/90/0] is composed of PVDF with material properties given in Table 1. The bottom and top surfaces are assumed to be electrically grounded. To compare the derived results with an exact solution (Heyliger, 1997) reproduced later by Lage et al.(2004), one should set $h = 0.01$ m and $p_0 = 3$ Pa.

The data listed in Tables 2 and 3 show that the SaS method permits us to find the 3D exact solution for thick piezoelectric laminated orthotropic plates with a prescribed accuracy by using a sufficiently large number of SaS. Fig. 2 presents distributions of transverse shear stresses, electric displacement and electric potential in the thickness direction for different values of the slenderness ratio $a/h$ employing seven SaS for each layer. These results demonstrate convincingly the high potential of the proposed piezoelectric plate formulation. This is due to the fact that boundary conditions

**Table 4**
Results for a piezoelectric three-ply plate with $a/h = 4$ under electric loading[c].

| Variable | Exact | $I_n = 3$ | $I_n = 5$ | $I_n = 7$ | $I_n = 9$ | $I_n = 11$ |
|---|---|---|---|---|---|---|
| $-u_1(0, a/2, 0.005) \times 10^{10}$, m | 3.223 | 3.1922 | 3.2226 | 3.2226 | 3.2226 | 3.2226 |
| $u_3(a/2, a/2, 0.005) \times 10^{9}$, m | 3.313 | 3.3089 | 3.3131 | 3.3131 | 3.3131 | 3.3131 |
| $\sigma_{22}(a/2, a/2, 0.01/6) \times 10^{-3}$, Pa | 2.841 | 2.8440 | 2.8408 | 2.8407 | 2.8407 | 2.8407 |
| $-\sigma_{12}(0, 0, 0.005) \times 10^{-2}$, Pa | 5.543 | 5.5174 | 5.5427 | 5.5427 | 5.5427 | 5.5427 |
| $\sigma_{13}(0, a/2, 0.003) \times 10^{-2}$, Pa | 2.925 | 2.4660 | 2.9315 | 2.9246 | 2.9246 | 2.9246 |
| $-\sigma_{23}(a/2, 0, 0.01/6) \times 10^{-2}$, Pa | 2.328 | 1.7841 | 2.3174 | 2.3283 | 2.3284 | 2.3284 |
| | | 2.0834 | 2.3258 | 2.3283 | 2.3284 | 2.3284 |
| $-\sigma_{33}(a/2, a/2, 0) \times 10^{-1}$, Pa | 3.629 | 3.9740 | 3.6034 | 3.6292 | 3.6290 | 3.6290 |
| $-D_1(0, a/2, 0.005) \times 10^{6}$, C/m$^2$ | 1.739 | 1.7393 | 1.7389 | 1.7389 | 1.7389 | 1.7389 |
| $-D_3(a/2, a/2, 0.005) \times 10^{6}$, C/m$^2$ | 3.100 | 3.0705 | 3.1002 | 3.1003 | 3.1003 | 3.1003 |

[c] Stress $\sigma_{23}$ is evaluated at the second layer interface $x_3^{[2]} = 0.01/6$.

on the bottom and top surfaces and continuity conditions at layer interfaces for transverse stress and electric displacement components are satisfied exactly utilizing the constitutive Eqs. (22) and (23). Additionally, we represent in Fig. 3 the logarithmic errors

$$\delta_1^{\pm} = \lg|\sigma_{13}(0,a/2,\pm h/2)|, \quad \delta_2^{\pm} = \lg|\sigma_{23}(a/2,0,\pm h/2)|,$$
$$\delta_3^{-} = \lg|\sigma_{33}(a/2,a/2,-h/2)|, \quad \delta_3^{+} = \lg|\sigma_{33}(a/2,a/2,h/2) - p_0|, \tag{33}$$

**Table 5**
Results for a piezoelectric three-ply plate with $a/h = 10$ under electric loading[d].

| Variable | Exact | $I_n = 3$ | $I_n = 5$ | $I_n = 7$ | $I_n = 9$ |
|---|---|---|---|---|---|
| $-u_1(0,a/2,0.005)\times 10^{10}$, m | 3.614 | 3.6127 | 3.6135 | 3.6135 | 3.6135 |
| $u_3(a/2,a/2,0.005)\times 10^{9}$, m | 3.117 | 3.1169 | 3.1173 | 3.1173 | 3.1173 |
| $\sigma_{22}(a/2,a/2,0.01/6)\times 10^{-3}$, Pa | 2.400 | 2.4035 | 2.4008 | 2.4008 | 2.4008 |
| $-\sigma_{12}(0,0,0.005)\times 10^{-2}$, Pa | 2.259 | 2.2590 | 2.2593 | 2.2593 | 2.2593 |
| $\sigma_{13}(0,a/2,0.01/6)\times 10^{-1}$, Pa | 7.734 | 7.7137 | 7.7330 | 7.7330 | 7.7330 |
| | | 8.7016 | 7.7374 | 7.7330 | 7.7330 |
| $-\sigma_{23}(a/2,0,0.01/6)\times 10^{-2}$, Pa | 1.223 | 1.1823 | 1.2231 | 1.2233 | 1.2233 |
| | | 1.2039 | 1.2232 | 1.2233 | 1.2233 |
| $\sigma_{33}(a/2,a/2,0)$, Pa | 2.208 | 1.0746 | 2.2184 | 2.2091 | 2.2091 |
| $-D_1(0,a/2,0.005)\times 10^{7}$, C/m$^2$ | 6.96 | 6.9559 | 6.9557 | 6.9557 | 6.9557 |
| $-D_3(a/2,a/2,0.005)\times 10^{6}$, C/m$^2$ | 2.412 | 2.4083 | 2.4123 | 2.4123 | 2.4123 |

[d] Stresses $\sigma_{13}$ and $\sigma_{23}$ are evaluated at the second layer interface $x_3^{[2]} = 0.01/6$.

which help to assess the accuracy of fulfilling the boundary conditions for transverse stresses on the bottom and top surfaces of the plate. It is necessary to note that the proposed SaS method provides a monotonic convergence that is impossible with *equally spaced* SaS (Kulikov and Plotnikova, 2011b).

### 5.2. Square piezoelectric three-layer plate under electric loading

Consider next the same square symmetric PVDF three-ply plate with the stacking sequence [0/90/0] subjected to electric loading

$$\varphi^{[0]} = 0, \quad \varphi^{[N]} = \varphi_0 \sin\frac{\pi x_1}{a}\sin\frac{\pi x_2}{b}. \tag{34}$$

The bottom and top surfaces of the plate are assumed to be traction free. The derived results are compared with an exact solution (Heyliger, 1997; Lage et al., 2004) in the case of choosing $h = 0.01$ m and $\varphi_0 = 200$ V.

Tables 4 and 5 demonstrate again the high potential of the piezoelectric laminated plate formulation developed. Fig. 4 shows the distributions of transverse shear stresses, electric displacement and electric potential in the thickness direction for different slenderness ratios employing seven SaS for each layer. It is seen that the boundary conditions on the bottom and top surfaces and continuity conditions at layer interfaces for transverse stresses and electric displacement are satisfied properly.

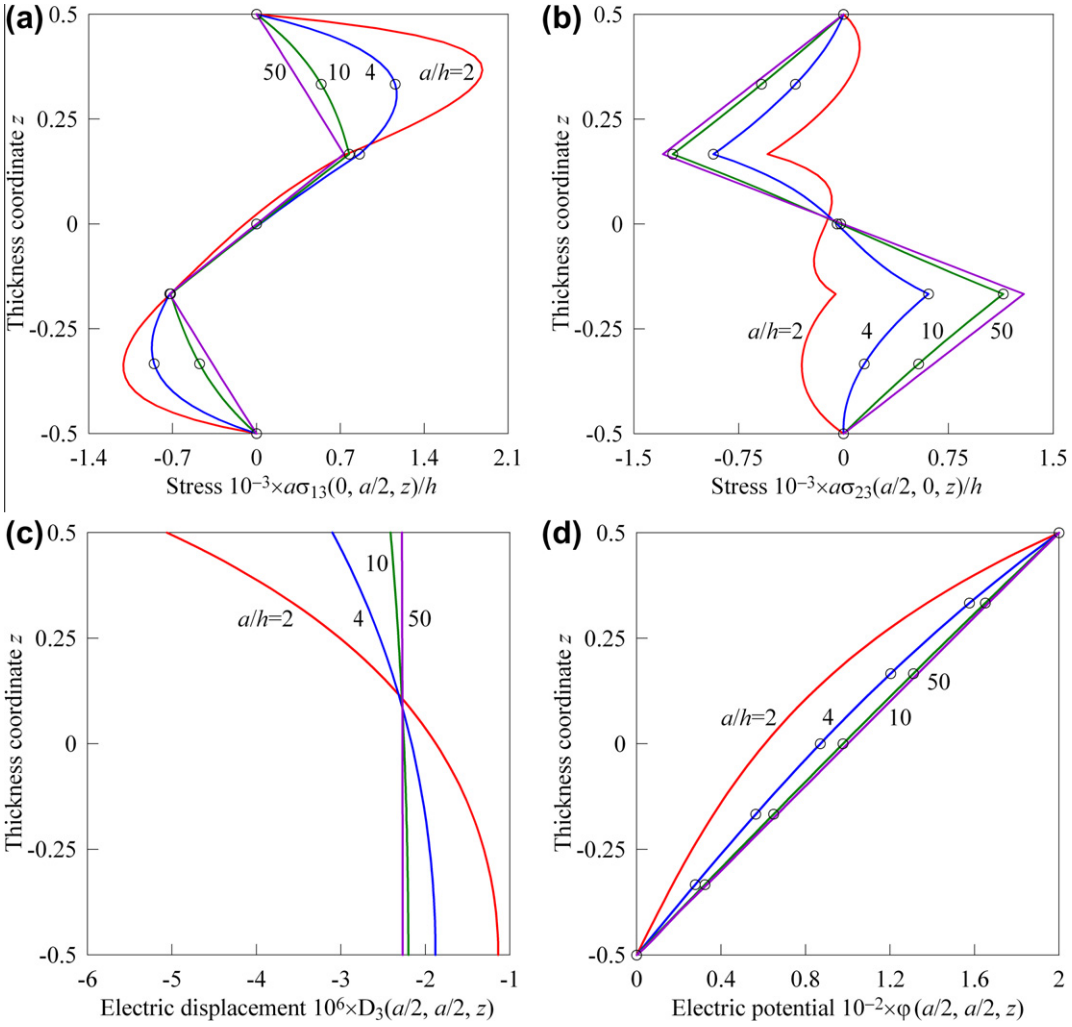


**Fig. 4.** Distributions of transverse shear stresses, electric displacement and electric potential through the thickness of the three-ply plate subjected to electric loading for $I_1 = I_2 = I_3 = 7$: present analysis (—) and Heyliger (○), where $z = x_3/h$.

## 6. 3D exact solution for piezoelectric anisotropic plates in cylindrical bending

Herein, we study a simply supported piezoelectric laminated anisotropic plate in cylindrical bending. The boundary conditions of the plate with electrically grounded edges are taken as

$$\sigma_{11}^{(n)} = \sigma_{12}^{(n)} = u_3^{(n)} = \varphi^{(n)} = 0 \quad \text{at } x_1 = 0 \text{ and } x_1 = a \tag{35}$$

to simulate simple supports, where $a$ is the width of the plate. In the case of a monoclinic piezoelectric material with poling direction coincident with the $x_3$ axis, we can search an analytical solution of the problem as follows:

**Table 6**
Results for an angle-ply plate with $a/h = 5$ under mechanical loading.

| $I_n$ | $U_1^{\mathrm{M}}(0.5)$ | $U_3^{\mathrm{M}}(0)$ | $S_{11}^{\mathrm{M}}(0.5)$ | $S_{13}^{\mathrm{M}}(0)$ | $S_{23}^{\mathrm{M}}(0.25)$ | $S_{33}^{\mathrm{M}}(0)$ | $\Phi^{\mathrm{M}}(-0.5)$ | $\Delta_3^{\mathrm{M}}(0.5)$ |
|---|---|---|---|---|---|---|---|---|
| 3 | −2.3687 | 3.0097 | 7.6031 | 0.39954 | −0.62340 | 0.50943 | −0.35169 | −0.34270 |
| 5 | −2.3693 | 3.0103 | 7.5999 | 0.40849 | −0.69302 | 0.51015 | −0.35177 | −0.34303 |
| 7 | −2.3693 | 3.0103 | 7.5999 | 0.40848 | −0.69289 | 0.51015 | −0.35177 | −0.34303 |
| 9 | −2.3693 | 3.0103 | 7.5999 | 0.40848 | −0.69289 | 0.51015 | −0.35177 | −0.34303 |
| Exact | −2.369 | 3.010 | 7.600 | 0.408 | −0.693 | 0.510 | −0.352 | −0.343 |

**Table 7**
Results for an angle-ply plate with $a/h = 10$ under mechanical loading.

| $I_n$ | $U_1^{\mathrm{M}}(0.5)$ | $U_3^{\mathrm{M}}(0)$ | $S_{11}^{\mathrm{M}}(0.5)$ | $S_{13}^{\mathrm{M}}(0)$ | $S_{23}^{\mathrm{M}}(0.25)$ | $S_{33}^{\mathrm{M}}(0)$ | $\Phi^{\mathrm{M}}(-0.5)$ | $\Delta_3^{\mathrm{M}}(0.5)$ |
|---|---|---|---|---|---|---|---|---|
| 3 | −2.1902 | 2.1579 | 6.8147 | 0.41082 | −0.76535 | 0.51150 | −0.33770 | −0.34552 |
| 5 | −2.1904 | 2.1580 | 6.8140 | 0.41867 | −0.82530 | 0.51222 | −0.33772 | −0.34560 |
| 7 | −2.1904 | 2.1580 | 6.8140 | 0.41866 | −0.82527 | 0.51222 | −0.33772 | −0.34560 |
| 9 | −2.1904 | 2.1580 | 6.8140 | 0.41866 | −0.82527 | 0.51222 | −0.33772 | −0.34560 |

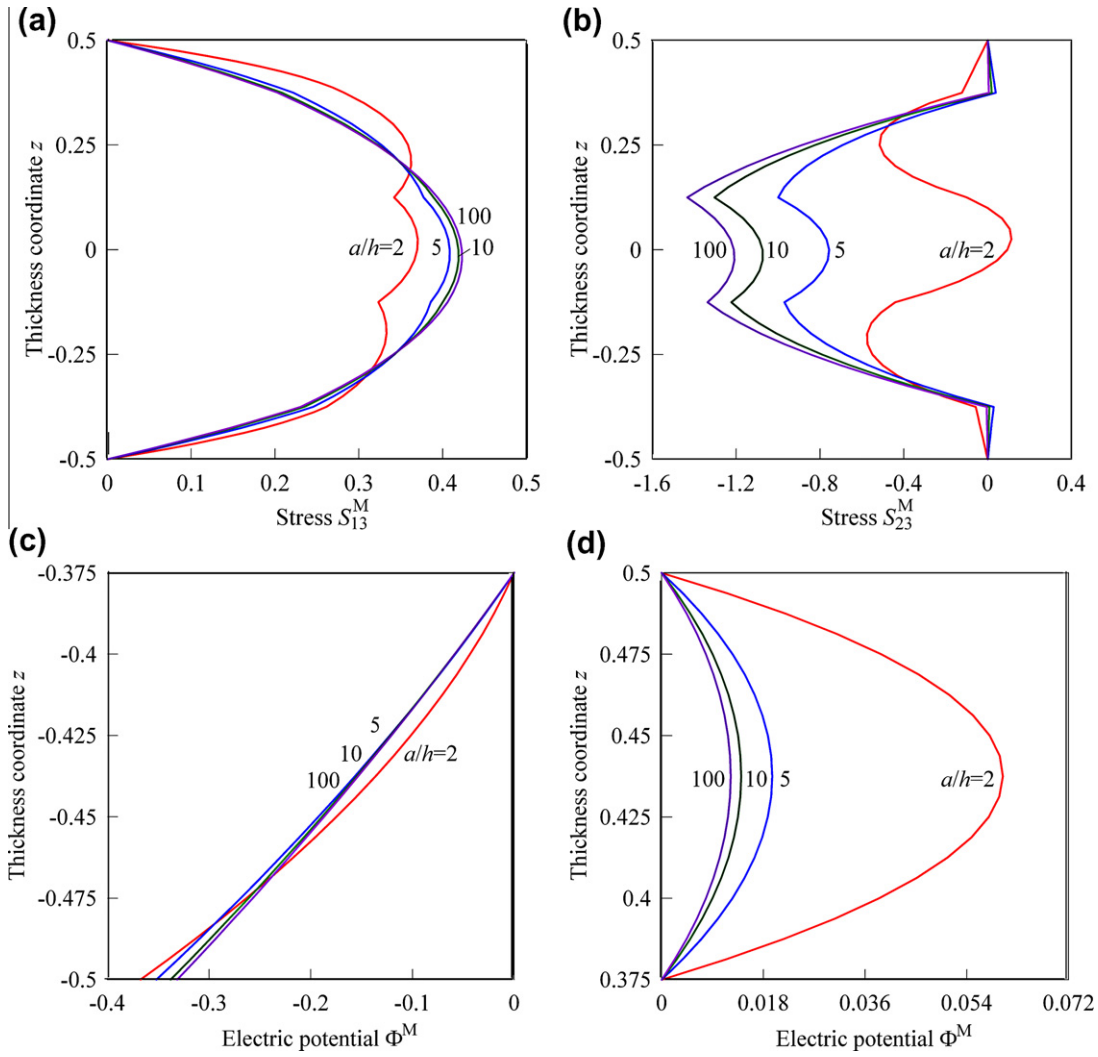


**Fig. 5.** Mechanical loading of the angle-ply plate: distributions of transverse shear stresses through the thickness of the plate and electric potential through the thicknesses of piezoelectric layers for $I_1 = I_2 = I_3 = I_4 = I_5 = 7$.

$$u_1^{(n)i_n} = \sum_{r=1}^{\infty} \overline{u}_{1r}^{(n)i_n} \cos\frac{r\pi x_1}{a}, \quad u_2^{(n)i_n} = \sum_{r=1}^{\infty} \overline{u}_{2r}^{(n)i_n} \cos\frac{r\pi x_1}{a},$$
$$u_3^{(n)i_n} = \sum_{r=1}^{\infty} \overline{u}_{3r}^{(n)i_n} \sin\frac{r\pi x_1}{a}, \quad \varphi^{(n)i_n} = \sum_{r=1}^{\infty} \overline{\varphi}_r^{(n)i_n} \sin\frac{r\pi x_1}{a}. \tag{36}$$

The external electromechanical loads are also expanded in Fourier series.

Substituting (36) and Fourier series corresponding to electromechanical loading into the extended potential energy (18) and (21) and allowing for (3), (7), (11), (12), (16), (24), and (25), one finds

$$\Pi = \sum_{r=1}^{\infty} \Pi_r \left( \overline{u}_{ir}^{(n)i_n}, \overline{\varphi}_r^{(n)i_n} \right). \tag{37}$$

The use of the variational Eq. (27) leads to a system of linear algebraic equations

$$\frac{\partial \Pi_r}{\partial \overline{u}_{ir}^{(n)i_n}} = 0, \quad \frac{\partial \Pi_r}{\partial \overline{\varphi}_r^{(n)i_n}} = 0 \tag{38}$$

of order $4\left(\sum_n I_n - N + 1\right)$. The linear system (38) can be solved by a method of Gaussian elimination.

The described algorithm was performed with the Symbolic Math Toolbox, which incorporates symbolic computations into the numeric environment of MATLAB. This gave the possibility to derive the exact solutions of 2D electroelasticity for laminated anisotropic plates with a specified accuracy.

### 6.1. Angle-ply plate with attached piezoelectric layers under mechanical loading

A symmetric three-ply plate with the stacking sequence [45/−45/45] is made of the graphite–epoxy composite and covered with PZT-5A layers of equal thicknesses on its bottom and top surfaces. This means that a five-ply plate with the stacking sequence [PZT5A/45/−45/45/PZT5A] is studied. The ply thicknesses are taken as $h_1 = h_5 = h/8$ and $h_2 = h_3 = h_4 = h/4$. The electromechanical properties of both materials are given in Table 1. The interfaces between the substrate and piezoelectric plies are electroded and grounded.

The boundary conditions at outer surfaces are written as

$$\sigma_{13}^{[0]} = \sigma_{13}^{[N]} = \sigma_{23}^{[0]} = \sigma_{23}^{[N]} = \sigma_{33}^{[0]} = 0, \quad \sigma_{33}^{[N]} = p_0 \sin\frac{\pi x_1}{a},$$
$$D_3^{[0]} = 0, \quad \varphi^{[N]} = 0. \tag{39}$$

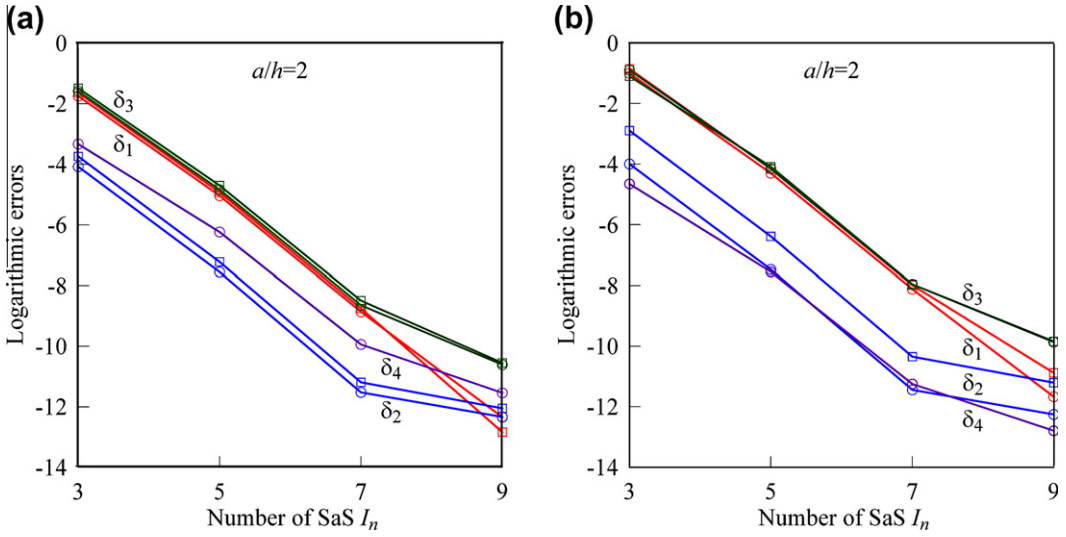


**Fig. 6.** Accuracy of satisfying the boundary conditions $\delta_i^-$, $\delta_4^-$ and $\delta_i^+$ on the bottom (○) and top (□) surfaces of the angle-ply plate: (a) mechanical loading and (b) electric loading.

**Table 8**
Results for an angle−ply plate with $a/h = 5$ under electric loading.

| $I_n$ | $U_1^E(0.5)$ | $U_3^E(0)$ | $S_{11}^E(0.5)$ | $S_{13}^E(0.4375)$ | $S_{23}^E(0.25)$ | $S_{33}^E(0)$ | $\Phi^E(-0.5)$ | $\Delta_3^E(0.5)$ |
|---|---|---|---|---|---|---|---|---|
| 3 | −6.2366 | 3.7450 | −1.4351 | −2.1627 | −1.6306 | 3.2910 | −0.028133 | −1.0863 |
| 5 | −6.2375 | 3.7459 | −1.4361 | −2.1276 | −1.7458 | 3.4768 | −0.028146 | −1.0868 |
| 7 | −6.2375 | 3.7459 | −1.4361 | −2.1276 | −1.7456 | 3.4765 | −0.028146 | −1.0868 |
| 9 | −6.2375 | 3.7459 | −1.4361 | −2.1276 | −1.7456 | 3.4765 | −0.028146 | −1.0868 |
| Exact | −6.238 | 3.746 | −1.436 | −2.128 | −1.746 | 3.477 | −0.028 | −1.087 |

**Table 9**
Results for an angle−ply plate with $a/h = 10$ under electric loading.

| $I_n$ | $U_1^E(0.5)$ | $U_3^E(0)$ | $S_{11}^E(0.5)$ | $S_{13}^E(0.4375)$ | $S_{23}^E(0.25)$ | $S_{33}^E(0)$ | $\Phi^E(-0.5)$ | $\Delta_3^E(0.5)$ |
|---|---|---|---|---|---|---|---|---|
| 3 | −5.7633 | 3.5369 | −1.5749 | −2.3430 | −2.0098 | 3.6076 | −0.029889 | −1.0770 |
| 5 | −5.7635 | 3.5371 | −1.5751 | −2.3113 | −2.1176 | 3.8167 | −0.029892 | −1.0771 |
| 7 | −5.7635 | 3.5371 | −1.5751 | −2.3113 | −2.1176 | 3.8166 | −0.029892 | −1.0771 |
| 9 | −5.7635 | 3.5371 | −1.5751 | −2.3113 | −2.1176 | 3.8166 | −0.029892 | −1.0771 |

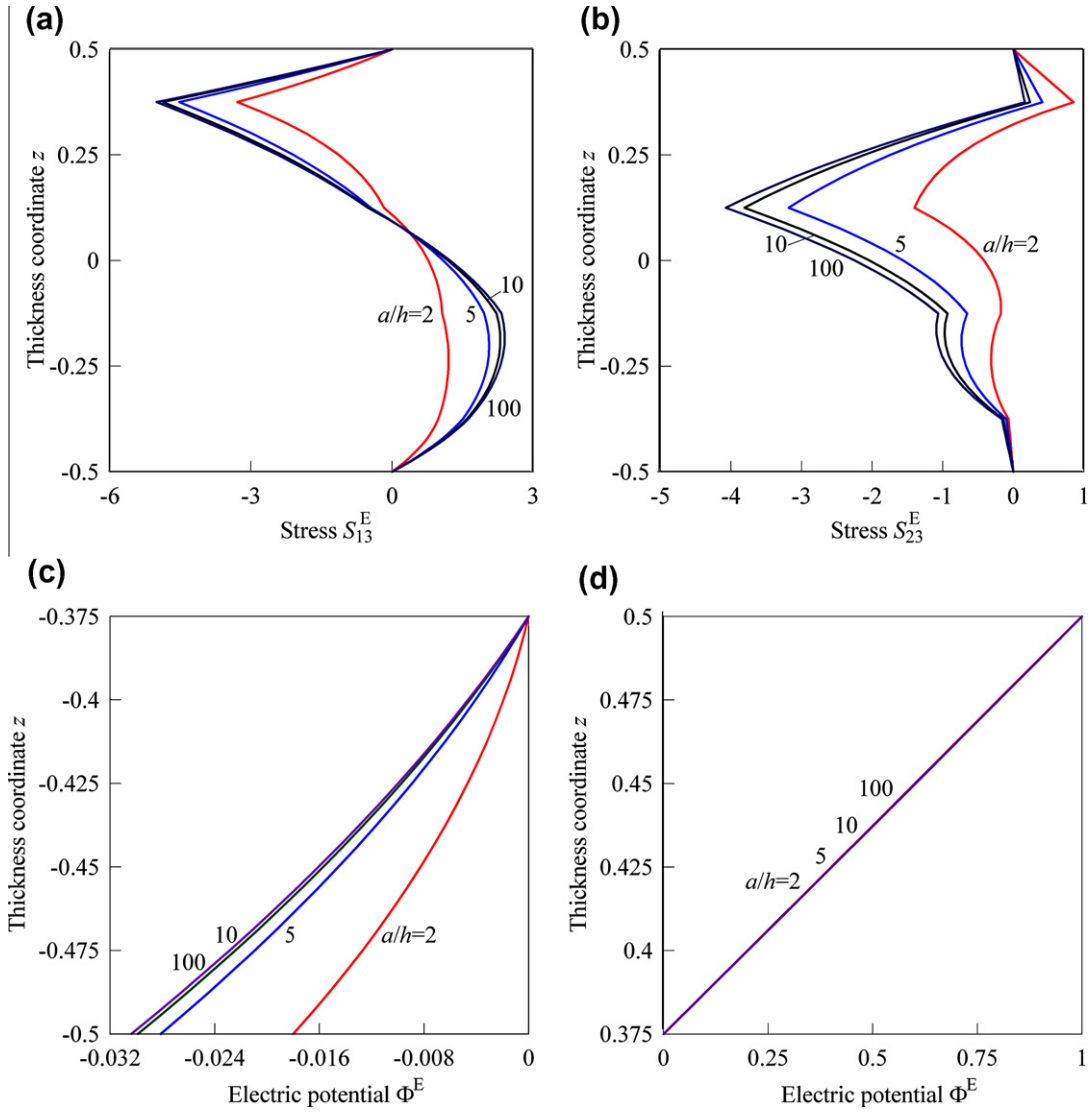


**Fig. 7.** Electric loading of the angle-ply plate: distributions of transverse shear stresses through the thickness of the plate and electric potential through the thicknesses of piezoelectric layers for $l_1 = l_2 = l_3 = l_4 = l_5 = 7$.

**Table 10**
Results for the unsymmetric angle-ply plate with $a/h = 4$ under mechanical loading.

| $l_n$ | $\overline{u}_1(-0.5)$ | $\overline{u}_3(-0.5)$ | $\overline{\sigma}_{11}(-0.5)$ | $\overline{\sigma}_{12}(-0.5)$ | $\overline{\sigma}_{13}(0.125)$ | $\overline{\sigma}_{23}(0.125)$ | $\overline{\varphi}(-0.5)$ | $\widetilde{\varphi}(-0.5)$ | $\overline{D}_3(0.25)$ |
|---|---|---|---|---|---|---|---|---|---|
| 3 | 1.1318 | 6.4450 | −4.8241 | 1.9546 | 7.3267 | 8.5498 | 2.5402 | −1.5100 | −4.1738 |
| 5 | 1.1328 | 6.4493 | −4.8174 | 1.9567 | 7.4820 | 8.8193 | 2.5433 | −1.5156 | −1.8940 |
| 7 | 1.1328 | 6.4493 | −4.8174 | 1.9567 | 7.4805 | 8.8168 | 2.5433 | −1.5156 | −1.8911 |
| 9 | 1.1328 | 6.4493 | −4.8174 | 1.9567 | 7.4805 | 8.8168 | 2.5433 | −1.5156 | −1.8911 |

**Table 11**
Results for the unsymmetric angle-ply plate with $a/h = 10$ under mechanical loading.

| $l_n$ | $\overline{u}_1(-0.5)$ | $\overline{u}_3(-0.5)$ | $\overline{\sigma}_{11}(-0.5)$ | $\overline{\sigma}_{12}(-0.5)$ | $\overline{\sigma}_{13}(0.125)$ | $\overline{\sigma}_{23}(0.125)$ | $\overline{\varphi}(-0.5)$ | $\widetilde{\varphi}(-0.5)$ | $\overline{D}_3(0.25)$ |
|---|---|---|---|---|---|---|---|---|---|
| 3 | 6.1680 | 49.156 | −23.645 | 9.7156 | 20.252 | 22.213 | 6.2089 | 5.8550 | −4.3957 |
| 5 | 6.1690 | 49.164 | −23.638 | 9.7170 | 20.654 | 22.887 | 6.2100 | 5.8557 | −2.1744 |
| 7 | 6.1690 | 49.164 | −23.638 | 9.7170 | 20.653 | 22.886 | 6.2100 | 5.8557 | −2.1741 |
| 9 | 6.1690 | 49.164 | −23.638 | 9.7170 | 20.653 | 22.886 | 6.2100 | 5.8557 | −2.1741 |

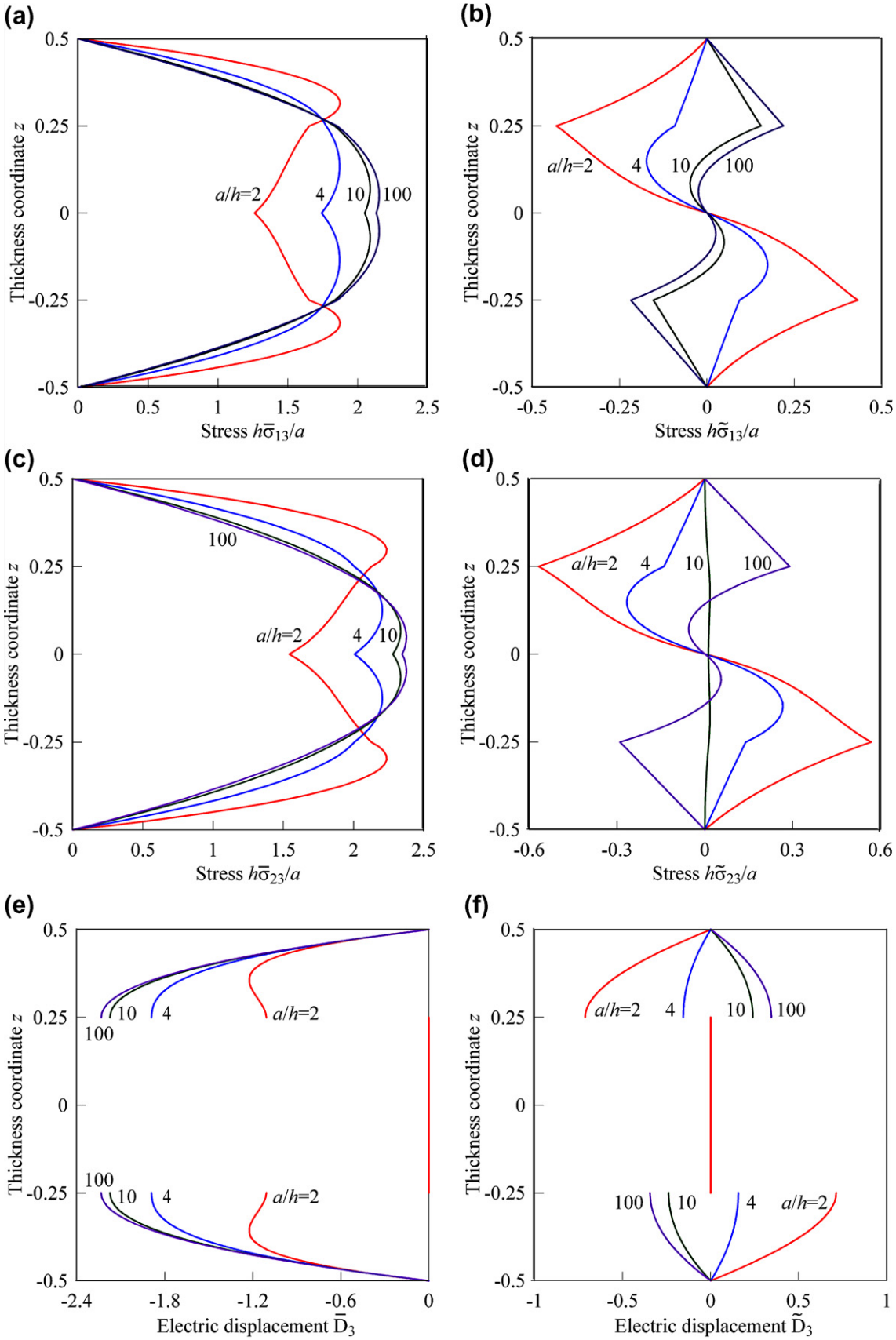


**Fig. 8.** Mechanical loading of the unsymmetric angle-ply plate: distributions of transverse shear stresses and electric displacement through the thickness of the plate for $I_1 = I_2 = I_3 = I_4 = 7$.

To compare the results derived with an exact solution (Vel and Batra, 2000a), we introduce dimensionless variables as follows:

$$U_1^{\mathrm{M}} = 100E_{\mathrm{T}}h^2u_1(a/4,z)/p_0a^3, \quad U_3^{\mathrm{M}} = 100E_{\mathrm{T}}h^3u_3(a/2,z)/p_0a^4,$$
$$S_{11}^{\mathrm{M}} = 10h^2\sigma_{11}(a/2,z)/p_0a^2, \quad S_{13}^{\mathrm{M}} = h\sigma_{13}(a/8,z)/p_0a,$$
$$S_{23}^{\mathrm{M}} = 10h\sigma_{23}(7a/8,z)/p_0a, \quad S_{33}^{\mathrm{M}} = \sigma_{33}(a/2,z)/p_0,$$
$$\Phi^{\mathrm{M}} = 100E_{\mathrm{T}}d_{\mathrm{T}}h\varphi(a/2,z)/p_0a^2, \quad \Delta_3^{\mathrm{M}} = h^2D_3(a/2,z)/d_{\mathrm{T}}p_0a^2, \tag{40}$$

where $E_{\mathrm{T}} = 10.3$ GPa, $d_{\mathrm{T}} = 374\times10^{-12}$ m/V and $z = x_3/h$.

The data listed in Tables 6 and 7 show that the SaS technique permits the derivation of exact solutions of plane strain electroelasticity for thick angle-ply plates with a prescribed accuracy using a sufficient number of SaS. Fig. 5 presents distributions of transverse shear stresses through the thickness of the plate and electric potential through the thicknesses of piezoelectric layers for different values of the slenderness ratio $a/h$ by choosing seven SaS for each layer. As can be seen, the boundary conditions on outer surfaces and continuity conditions at layer interfaces for transverse shear stresses are satisfied with a high accuracy. This statement is confirmed convincingly in Fig. 6(a) by means of logarithmic errors

$$\delta_\alpha^{\pm} = \lg\left|S_{\alpha3}^{\mathrm{M}}(\pm0.5)\right|, \quad \delta_3^{-} = \lg\left|S_{33}^{\mathrm{M}}(-0.5)\right|,$$
$$\delta_3^{+} = \lg\left|S_{33}^{\mathrm{M}}(0.5)-1\right|, \quad \delta_4^{-} = \lg\left|\Delta_3^{\mathrm{M}}(-0.5)\right|, \tag{41}$$

which characterize the accuracy of fulfilling the boundary conditions for transverse stress components on the bottom and top surfaces of the thick plate and the transverse component of the electric displacement on the bottom surface as well.

### 6.2. Angle-ply plate with attached piezoelectric layers under electric loading

Next, we study the case of electric loading of the same three-ply graphite–epoxy plate covered by PZT-5A layers and consider boundary conditions at outer surfaces as follows:

$$\sigma_{13}^{[0]} = \sigma_{13}^{[N]} = \sigma_{23}^{[0]} = \sigma_{23}^{[N]} = \sigma_{33}^{[0]} = \sigma_{33}^{[N]} = 0,$$
$$D_3^{[0]} = 0, \quad \varphi^{[N]} = \varphi_0\sin\frac{\pi x_1}{a}. \tag{42}$$

In order to compare the results with an exact solution of Vel and Batra (2000a), the following dimensionless variables should be introduced:

$$U_1^{\mathrm{E}} = 10hu_1(a/4,z)/ad_{\mathrm{T}}\varphi_0, \quad U_3^{\mathrm{E}} = 10h^2u_3(a/2,z)/a^2d_{\mathrm{T}}\varphi_0,$$
$$S_{11}^{\mathrm{E}} = h\sigma_{11}(a/2,z)/10E_{\mathrm{T}}d_{\mathrm{T}}\varphi_0, \quad S_{13}^{\mathrm{E}} = a\sigma_{13}(a/4,z)/E_{\mathrm{T}}d_{\mathrm{T}}\varphi_0,$$
$$S_{23}^{\mathrm{E}} = a\sigma_{23}(7a/8,z)/E_{\mathrm{T}}d_{\mathrm{T}}\varphi_0, \quad S_{33}^{\mathrm{E}} = a^2\sigma_{33}(a/2,z)/hE_{\mathrm{T}}d_{\mathrm{T}}\varphi_0,$$
$$\Phi^{\mathrm{E}} = \varphi(a/2,z)/\varphi_0, \quad \Delta_3^{\mathrm{E}} = hD_3(a/2,z)/100E_{\mathrm{T}}d_{\mathrm{T}}^2\varphi_0, \quad z = x_3/h. \tag{43}$$

Tables 8 and 9 demonstrate again the high potential of the piezoelectric laminated plate formulation developed. Fig. 7 shows distributions of transverse shear stresses through the thickness of the plate and electric potential through the thicknesses of piezoelectric layers employing seven SaS for each layer. It is seen that the boundary conditions on outer surfaces and continuity conditions at layer interfaces for transverse shear stresses are satisfied correctly. Additionally, we represent in Fig. 6(b) the logarithmic errors

$$\delta_i^{\pm} = \lg\left|S_{i3}^{\mathrm{E}}(\pm0.5)\right|, \quad \delta_4^{-} = \lg\left|\Delta_3^{\mathrm{E}}(-0.5)\right|, \tag{44}$$

which help to assess the accuracy of fulfilling the boundary conditions for transverse stress and electric displacement components on outer surfaces of a thick plate. It should be mentioned that the proposed SaS method also provides the uniform convergence for piezoelectric angle-ply plates in cylindrical bending subjected to mechanical and electric loads.

## 7. 3D exact solution for antisymmetric piezoelectric angle-ply plates

Consider a simply supported antisymmetric angle-ply rectangular plate subjected to sinusoidally distributed transverse loading

$$p_1^{-} = p_1^{+} = p_2^{-} = p_2^{+} = p_3^{-} = 0,$$
$$p_3^{-} = -\frac{1}{2}p_0\sin\frac{r\pi x_1}{a}\sin\frac{s\pi x_2}{b}, \quad p_3^{+} = \frac{1}{2}p_0\sin\frac{r\pi x_1}{a}\sin\frac{s\pi x_2}{b} \tag{45}$$

or sinusoidal electric loading

$$\varphi^{[0]} = -\frac{1}{2}\varphi_0\sin\frac{r\pi x_1}{a}\sin\frac{s\pi x_2}{b}, \quad \varphi^{[N]} = \frac{1}{2}\varphi_0\sin\frac{r\pi x_1}{a}\sin\frac{s\pi x_2}{b} \quad (r,s\in N). \tag{46}$$

It is well established (Noor and Burton, 1990; Savoia and Reddy, 1992) that we can search an analytical solution of the problem in the following form:

$$u_1^{(n)i_n} = \overline{u}_{10}^{(n)i_n}\cos\frac{r\pi x_1}{a}\sin\frac{s\pi x_2}{b} + \widetilde{u}_{10}^{(n)i_n}\sin\frac{r\pi x_1}{a}\cos\frac{s\pi x_2}{b},$$
$$u_2^{(n)i_n} = \overline{u}_{20}^{(n)i_n}\sin\frac{r\pi x_1}{a}\cos\frac{s\pi x_2}{b} + \widetilde{u}_{20}^{(n)i_n}\cos\frac{r\pi x_1}{a}\sin\frac{s\pi x_2}{b},$$
$$u_3^{(n)i_n} = \overline{u}_{30}^{(n)i_n}\sin\frac{r\pi x_1}{a}\sin\frac{s\pi x_2}{b} + \widetilde{u}_{30}^{(n)i_n}\cos\frac{r\pi x_1}{a}\cos\frac{s\pi x_2}{b},$$
$$\varphi^{(n)i_n} = \overline{\varphi}_0^{(n)i_n}\sin\frac{r\pi x_1}{a}\sin\frac{s\pi x_2}{b} + \widetilde{\varphi}_0^{(n)i_n}\cos\frac{r\pi x_1}{a}\cos\frac{s\pi x_2}{b}. \tag{47}$$

Substituting (45)–(47) in the total potential energy (18) and (21) and allowing for (3), (7), (11), (12), (16), (24), and (25), we have

$$\Pi = \Pi\left(\overline{u}_{i0}^{(n)i_n}, \widetilde{u}_{i0}^{(n)i_n}, \overline{\varphi}_0^{(n)i_n}, \widetilde{\varphi}_0^{(n)i_n}\right) \tag{48}$$

**Table 12**
Results for the unsymmetric angle-ply plate with $a/h = 4$ under electric loading.

| $I_n$ | $\overline{u}_1(-0.5)$ | $\overline{u}_3(-0.5)$ | $\overline{\sigma}_{11}(-0.5)$ | $\overline{\sigma}_{12}(-0.5)$ | $\overline{\sigma}_{13}(0.125)$ | $\widetilde{\sigma}_{13}(0.125)$ | $\overline{\sigma}_{23}(0.125)$ | $\widetilde{\sigma}_{23}(0.125)$ | $\overline{D}_3(0.25)$ |
|---|---|---|---|---|---|---|---|---|---|
| 5 | 35.268 | 90.078 | 25.657 | 52.285 | 1.8363 | −2.6948 | 18.563 | −7.2148 | −17212 |
| 7 | 35.268 | 90.078 | 25.657 | 52.285 | 1.7915 | −2.6507 | 18.487 | −7.1405 | −17213 |
| 9 | 35.268 | 90.078 | 25.657 | 52.285 | 1.7917 | −2.6508 | 18.488 | −7.1407 | −17213 |

**Table 13**
Results for the unsymmetric angle-ply plate with $a/h = 10$ under electric loading.

| $I_n$ | $\overline{u}_1(-0.5)$ | $\overline{u}_3(-0.5)$ | $\overline{\sigma}_{11}(-0.5)$ | $\overline{\sigma}_{12}(-0.5)$ | $\overline{\sigma}_{13}(0.125)$ | $\widetilde{\sigma}_{13}(0.125)$ | $\overline{\sigma}_{23}(0.125)$ | $\widetilde{\sigma}_{23}(0.125)$ | $\overline{D}_3(0.25)$ |
|---|---|---|---|---|---|---|---|---|---|
| 5 | 85.243 | 541.91 | 64.404 | 128.91 | −0.52030 | −1.2129 | 22.912 | −5.6276 | −43336 |
| 7 | 85.243 | 541.91 | 64.404 | 128.91 | −0.52780 | −1.2055 | 22.899 | −5.6151 | −43336 |
| 9 | 85.243 | 541.91 | 64.404 | 128.91 | −0.52780 | −1.2055 | 22.899 | −5.6151 | −43336 |

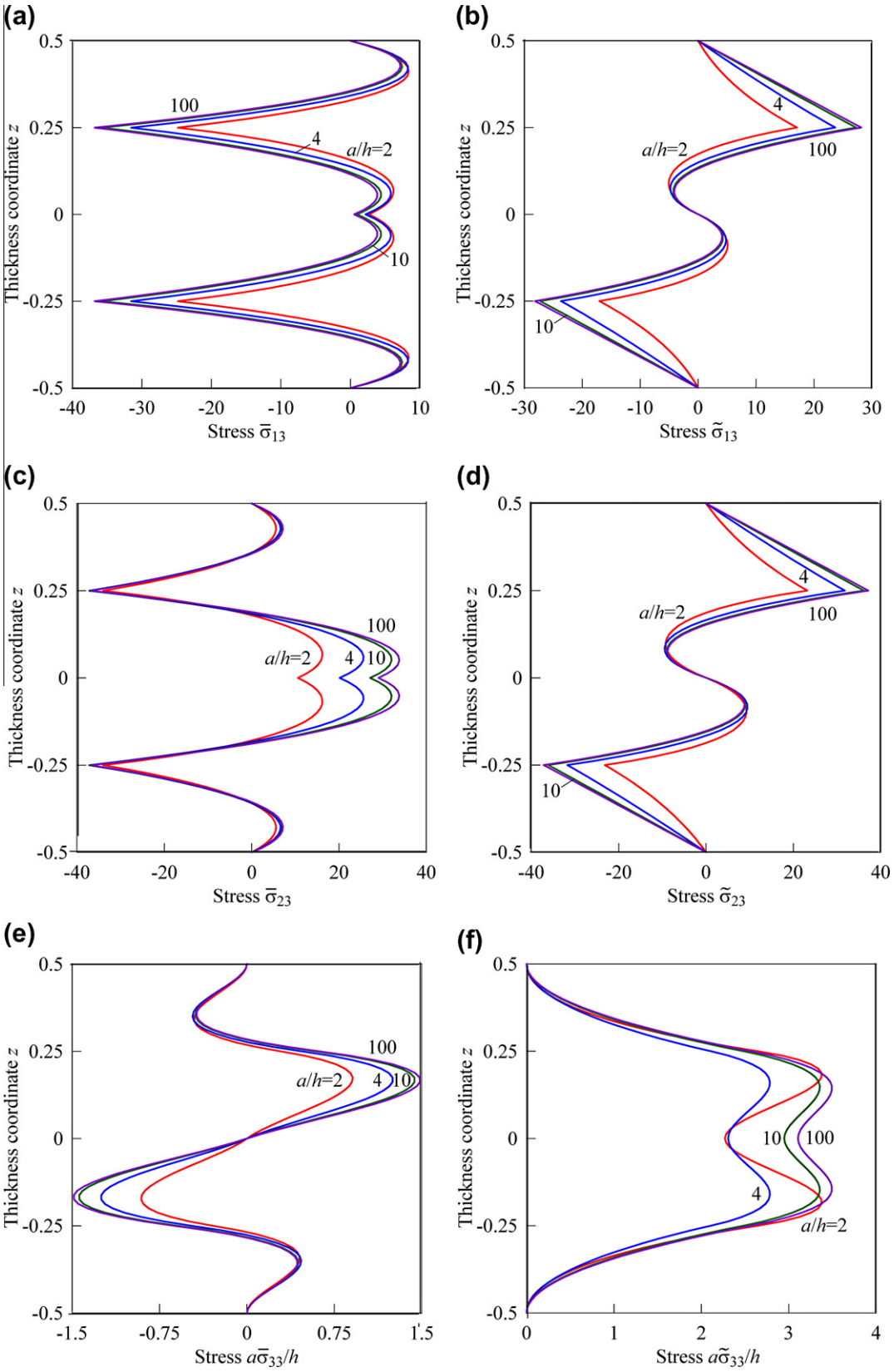


**Fig. 9.** Electric loading of the unsymmetric angle-ply plate: distributions of transverse stresses through the thickness of the plate for $I_1 = I_2 = I_3 = I_4 = 7$.

Invoking further the variational Eq. (27), one arrives at the system of linear algebraic equations

$$\frac{\partial \Pi}{\partial \overline{u}_{i0}^{(n)i_n}} = 0, \quad \frac{\partial \Pi}{\partial \widetilde{u}_{i0}^{(n)i_n}} = 0, \quad \frac{\partial \Pi}{\partial \overline{\varphi}_{0}^{(n)i_n}} = 0, \quad \frac{\partial \Pi}{\partial \widetilde{\varphi}_{0}^{(n)i_n}} = 0 \tag{49}$$

of order $8\left(\sum_n I_n - N + 1\right)$. The linear system (49) is solved by a method of Gaussian elimination. As accepted in this paper, the described algorithm was performed with the Symbolic Math Toolbox of MATLAB.

### 7.1. Unsymmetric angle-ply plate with attached PZT layers under mechanical loading

We study first a two-ply square plate [60/−60] composed of the graphite–epoxy composite with PZT layers bonded to its bottom and top surfaces and polarized in opposite directions parallel to the thickness coordinate. Thus, a four-ply plate with the stacking sequence [PZT/60/−60/PZT] is considered. The ply thicknesses are taken to be $h_n = h/4$, where $n = 1, 2, 3, 4$. The electromechanical properties of both materials are given in Table 1. It is assumed that the interfaces between PZT layers and a substrate are electroded and grounded. The plate is subjected to the transverse load distributed according to (45) with $r = s = 1$ and $p_0 = 1$ Pa. The boundary conditions concerning the electric field are

$$D_3^{[0]} = 0, \quad D_3^{[N]} = 0. \tag{50}$$

For further analysis it is convenient to introduce the following variables:

$$\begin{aligned}
&\overline{u}_1 = 10^{11} \times u_1(0, a/2, z), \quad \overline{u}_3 = 10^{11} \times u_3(a/2, a/2, z),\\
&\overline{\sigma}_{11} = \sigma_{11}(a/2, a/2, z), \quad \overline{\sigma}_{12} = \sigma_{12}(0, 0, z),\\
&\overline{\sigma}_{13} = 10\sigma_{13}(0, a/2, z), \quad \widetilde{\sigma}_{13} = 10\sigma_{13}(a/2, 0, z),\\
&\overline{\sigma}_{23} = 10\sigma_{23}(a/2, 0, z), \quad \widetilde{\sigma}_{23} = 10\sigma_{23}(0, a/2, z),\\
&\overline{\sigma}_{33} = \sigma_{33}(a/2, a/2, z), \quad \widetilde{\sigma}_{33} = \sigma_{33}(0, 0, z),\\
&\overline{\varphi} = 10^3 \times \varphi(a/2, a/2, z), \quad \widetilde{\varphi} = 10^4 \times \varphi(0, 0, z),\\
&\overline{D}_3 = 10^{11} \times D_3(a/2, a/2, z), \quad \widetilde{D}_3 = 10^{11} \times D_3(0, 0, z),\\
&z = x_3/h.
\end{aligned} \tag{51}$$

Tables 10 and 11 show that the proposed formulation based on the SaS method can be applied efficiently to derivation of 3D exact solutions of electroelasticity for unsymmetric angle-ply plates. Fig. 8 displays the distributions of transverse shear stresses and electric displacement in the thickness direction for different slenderness ratios choosing seven SaS for each layer.

### 7.2. Unsymmetric angle-ply plate with attached PZT layers under electric loading

Finally, we consider a similar square plate [60/−60] made of the graphite–epoxy composite with PZT layers attached to its outer surfaces and polarized in opposite directions parallel to the thickness coordinate. It is also assumed that the interfaces between the substrate and PZT layers are electroded and grounded. The plate is subjected to electric loading distributed according to (46) with $r = s = 1$ and $\varphi_0 = 1$ V.

Tables 12 and 13 list the results of the convergence study by using a various number of SaS for thick plates. Fig. 9 presents the distributions of transverse stress components in the thickness direction for different slenderness ratios employing again seven SaS for each layer.

## 8. Conclusions

An efficient method of solving the static problems of 3D electroelasticity for piezoelectric laminated plates has been proposed. It is based on the new method of SaS located at the Chebyshev polynomial nodes inside the plate body and layer interfaces as well. The stress analysis of piezoelectric plates is based on the 3D constitutive equations and gives an opportunity to obtain the 3D exact solutions of electroelasticity for thick and thin piezoelectric cross-ply and angle-ply plates with a prescribed accuracy.

## Acknowledgement

This work was supported by Russian Ministry of Education and Science under Grant No. 1.472.2011.

## References

Benjeddou, A., Deú, J.F., 2001. Piezoelectric transverse shear actuation and sensing of plates. Part 1: a three-dimensional mixed state space formulation. J. Intell. Mater. Syst. Struct. 12, 435–449.
Bisegna, P., Maceri, F., 1996. An exact three-dimensional solution for simply supported rectangular piezoelectric plates. J. Appl. Mech. 63, 628–638.
Burden, R.L., Faires, J.D., 2010. Numerical Analysis, ninth ed. Brooks/Cole, Cengage Learning, Boston.
Carrera, E., 2002. Theories and finite elements for multilayered, anisotropic, composite plates and shells. Arch. Comput. Meth. Eng. 9, 1–60.
Carrera, E., 2003. Theories and finite elements for multilayered plates and shells: a unified compact formulation with numerical assessment and benchmarking. Arch. Comput. Meth. Eng. 10, 215–296.
Carrera, E., Brischetto, S., Nali, P., 2011. Plates and Shells for Smart Structures: Classical and Advanced Theories for Modeling and Analysis. John Wiley & Sons Ltd.
Cheng, Z.Q., Batra, R.C., 2000. Three-dimensional asymptotic analysis of multiple-electroded piezoelectric laminates. AIAA J. 38, 317–324.
Cheng, Z.Q., Lim, C.W., Kitipornchai, S., 2000. Three-dimensional asymptotic approach to inhomogeneous and laminated piezoelectric plates. Int. J. Solids Struct. 37, 3153–3175.
Heyliger, P., 1994. Static behavior of laminated elastic/piezoelectric plates. AIAA J. 32, 2481–2484.
Heyliger, P., 1997. Exact solutions for simply supported laminated piezoelectric plates. J. Appl. Mech. 64, 299–306.
Heyliger, P., Brooks, S., 1996. Exact solutions for laminated piezoelectric plates in cylindrical bending. J. Appl. Mech. 63, 903–910.
Kapuria, S., Dumir, P.C., Sengupta, S., 1999. Three-dimensional solution for shape control of a simply supported rectangular hybrid plate. J. Therm. Stresses 22, 159–176.
Kalamkarov, A.L., Kolpakov, A.G., 2001. A new asymptotic model for a composite piezoelastic plate. Int. J. Solids Struct. 38, 6027–6044.
Kulikov, G.M., Plotnikova, S.V., 2008. Geometrically exact four-node piezoelectric solid-shell element. Mech. Adv. Mater. Struct. 15, 199–207.
Kulikov, G.M., Plotnikova, S.V., 2011a. Finite rotation piezoelectric exact geometry solid-shell element with nine degrees of freedom per node. Comput. Mater. Con. 23, 233–264.
Kulikov, G.M., Plotnikova, S.V., 2011b. Solution of statics problems for a three-dimensional elastic shell. Dokl. Phys. 56, 448–451.
Kulikov, G.M., Plotnikova, S.V., 2012a. Exact 3D stress analysis of laminated composite plates by sampling surfaces method. Compos. Struct. 94, 3654–3663.
Kulikov, G.M., Plotnikova, S.V., 2012b. On the use of sampling surfaces method for solution of 3D elasticity problems for thick shells. ZAMM – J. Appl. Math. Mech. 92, 910–920.
Kulikov, G.M., Plotnikova, S.V., 2013. Advanced formulation for laminated composite shells: 3D stress analysis and rigid-body motions. Compos. Struct. 95, 236–246.
Lage, R.G., Soares, C.M.M., Soares, C.A.M., Reddy, J.N., 2004. Modelling of piezolaminated plates using layerwise mixed finite elements. Comput. Struct. 82, 1849–1863.
Lee, J.S., Jiang, L.Z., 1996. Exact electroelastic analysis of piezoelectric laminae via state space approach. Int. J. Solids Struct. 33, 977–990.
Noor, A.K., Burton, W.S., 1990. Three-dimensional solutions for antisymmetrically laminated anisotropic plates. J. Appl. Mech. 57, 182–188.
Pagano, N.J., 1969. Exact solutions for composite laminates in cylindrical bending. J. Compos. Mater. 3, 398–411.
Pagano, N.J., 1970a. Exact solutions for rectangular bidirectional composites and sandwich plates. J. Compos. Mater. 4, 20–34.
Pagano, N.J., 1970b. Influence of shear coupling in cylindrical bending of anisotropic laminates. J. Compos. Mater. 4, 330–343.
Ray, M.C., Rao, K.M., Samanta, B., 1992. Exact analysis of coupled electroelastic behaviour of a piezoelectric plate under cylindrical bending. Comput. Struct. 45, 667–677.

Ray, M.C., Rao, K.M., Samanta, B., 1993. Exact solution for static analysis of an intelligent structure under cylindrical bending. Comput. Struct. 47, 1031–1042.

Reddy, J.N., Cheng, Z.Q., 2001. Three-dimensional solutions of smart functionally graded plates. J. Appl. Mech. 68, 234–241.

Savoia, M., Reddy, J.N., 1992. A variational approach to three-dimensional elasticity solutions of laminated composite plates. J. Appl. Mech. 59, S166–S175.

Tarn, J.Q., 2002. A state space formalism for piezothermoelasticity. Int. J. Solids Struct. 39, 5173–5184.

Tauchert, T.R., Ashida, F., Noda, N., Adali, S., Verijenko, V., 2000. Developments in thermopiezoelasticity with relevance to smart composite structures. Compos. Struct. 48, 31–38.

Tzou, H.S., 1993. Piezoelectric Shells: Distributed Sensing and Control of Continua. Kluwer-Academic, Dordrecht.

Vel, S.S., Batra, R.C., 2000a. Cylindrical bending of laminated plates with distributed and segmented piezoelectric actuators/sensors. AIAA J. 38, 857–867.

Vel, S.S., Batra, R.C., 2000b. Three-dimensional analytical solution for hybrid multilayered piezoelectric plates. J. Appl. Mech. 67, 558–567.

Vetyukov, Yu., Kuzin, A., Krommer, M., 2011. Asymptotic splitting in the three-dimensional problem of elasticity for non-homogeneous piezoelectric plates. Int. J. Solids Struct. 48, 12–23.

Vlasov, B.F., 1957. On the bending of rectangular thick plate. Trans. Moscow State Univ. 2, 25–31.

Wu, C.P., Chiu, K.H., Wang, Y.M., 2008. A review on the three-dimensional analytical approaches of multilayered and functionally graded piezoelectric plates and shells. Comput. Mater. Con. 8, 93–132.

Zhong, Z., Shang, E.T., 2003. Three-dimensional exact analysis of a simply supported functionally gradient piezoelectric plate. Int. J. Solids Struct. 40, 5335–5352.